A Transparent Medium to Provide a Visual Interpretation of Saturated/Unsaturated Hydraulic Behaviour

Peters, S.B.[1], Siemens, G.A.[1], Take, W.A.[2] and Ezzein, F.[1]
[1]*Department of Civil Engineering - Royal Military College of Canada, GeoEngineering Centre at Queen's-RMC, Kingston, Ontario, Canada*
[2]*Department of Civil Engineering - Queen's University, GeoEngineering Centre at Queen's-RMC, Kingston, Ontario, Canada*

ABSTRACT
Traditional laboratory testing of soil is limited by the inability to visually observe the behaviour within the soil mass and rely solely on instrumentation. To overcome this problem a soil-fluid combination was formed by matching their respective refractive indices to produce a transparent soil. At 100% saturation the soil-fluid combination is transparent. At degrees of saturation less than 100%, the soil particles and the air-fluid interfaces between the particles become visible. Transparent soil was used in this study with the aid of digital photography to identify the behaviour within the soil mass during the drainage process of a 1-D column apparatus. Results are presented to demonstrate the usefulness of transparent soil to interpret this behaviour.

RÉSUMÉ
Les essais traditionnels de laboratoire sur les sols non saturés et sur les systèmes d'eau ont été limités par le fait qu'il n'était pas possible d'observer visuellement la migration du front d'air sans le recours à l'instrumentation. Pour résoudre ce problème, un mélange sol-fluide est formé en combinant leurs indices de réfractions respectifs afin de produire le sol transparent. A un degré de saturation de 100%, le sol est transparent. A des degrés de saturation inférieurs à 100%, les interfaces air-fluide entre les particules deviennent visibles. Le sol transparent était utilisé avec l'aide de la photographie digitale afin d'identifier le comportement de ces interfaces durant le processus de séchage dans une colonne 1-D. Les résultats sont présentés pour démontrer l'utilité des sols transparents.

1 INTRODUCTION AND BACKGROUND

The amount of water in the unsaturated zone above the water table fluctuates in response to precipitation events and seasonal changes in the availability of moisture. The movement of water is significant in the unsaturated zone since it comprises of the transition zone from the atmosphere to the groundwater in the underlying aquifers. Several authors have studied water infiltration in soils through field tests, laboratory experiments and numerical modeling.

The typical experimental apparatus used to study the 1D hydraulic behaviour of infiltration in soils is the 1D column apparatus (Ho 2000, Bathurst et al. 2007, Yang et al. 2004a, Nahlawi et al. 2007). Results were reported in Yang et al. (2004b and 2006) for two layered soil columns of fine over coarser materials to study the effect of capillary barriers and the effect of rainfall intensity and duration, respectively.

An additional study was completed by Nahlawi et al. (2007) for a 1D soil column apparatus to investigate the unsaturated hydraulic behaviour of a layered soil-geotextile system under surface water infiltration. Ho (2000) and Bathurst et al. (2007) provide details and results of a 1D column apparatus of a sand-geotextile system to interpret the unsaturated hydraulic response under surface ponding.

Traditional laboratory testing of unsaturated soil has been limited by the inability to visually observe the wetting front migration and relied solely on installed instrumentation. At times the data resulted in values not consistent with predictions. An example includes sensors installed along a profile registering out of sequence. This could be due to time lags or fingering mechanisms along preferential flow paths.

The inability to visually interpret soil behaviour within the soil mass has led researchers to seek new testing methods to help explain the sometimes confusing data retrieved from the installed instrumentation. One potential method which could be used to overcome this problem is to use a transparent soil. This technique is achieved by matching the refractive index of a solid and a fluid. At 100% saturation the soil-fluid combination is transparent, as shown in Figure 1. In theory this method should produce a perfectly transparent soil but in practice there is a limited depth to which one can see into the mixture. Limiting factors that can create imperfections in a transparent mixture can include entrapped air bubbles, variations of index of refraction of the solids or by changes in the index of refraction of the fluid with time and environment.

Several transparent soils have been researched with successful results. Silica gels and amorphous silica have been investigated by Iskander et al. (2002a, 2002b and 2002c), Sadek et al. 2002, Welker et al. (1999), Liu et al. 2003, Gill and Lehane (2001) and Stanier et al. (2007) to model clay and sand particles. The focus of this research has been to measure deformation patterns, permeability

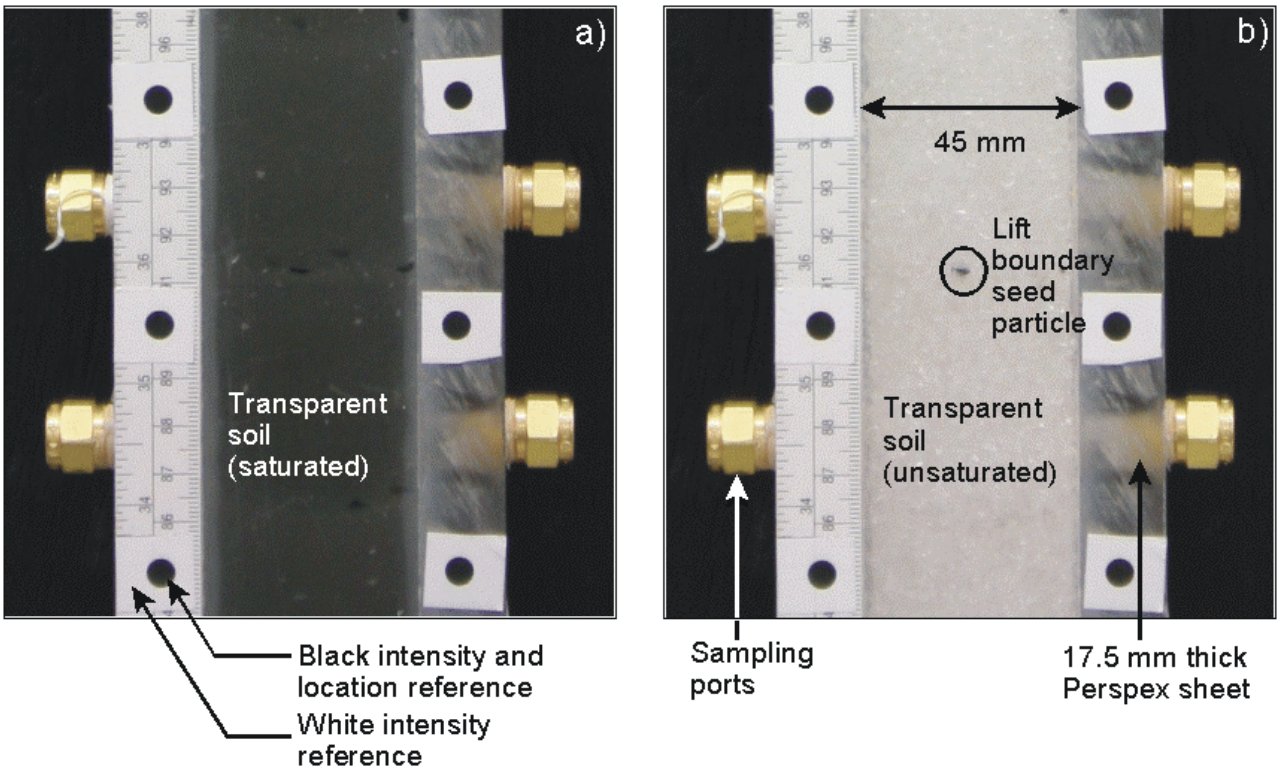

Figure1. Transparent soil a) saturated and b) unsaturated

and flow characteristics of the transparent medium. A second material, Aquabeads, was used by Lo et al. (2008) to measure multi-phase flow and surfactant flushing.

This paper will expand the use of transparent soils to investigate the use of transparency to interpret the results of a 1D column apparatus during the drying process through gravity drainage. Figure 1 shows the contrast between the saturated and unsaturated transparency of the soil. The first image (Figure 1a) shows the saturated soil and the second image (Figure 1b) shows the soil in an unsaturated state. The transparency of the saturated soil allows the ability to see the black background though the soil particles. The focus of this paper will be identifying the transition from saturated to unsaturated conditions and quantifying the flow. The air front migration will be analysed and mapped with the aid of digital photography and photo analysis software.

2 EXPERIMENTAL APPARATUS

2.1 1D Column Apparatus

The experimental equipment developed in this study was a 1400 mm tall column test apparatus. Figure 2 shows a schematic view of a column configuration for a typical drainage test. The square column was constructed with transparent Perspex walls with a thickness of 17.5 mm. The internal cross-sectional area is 2025 mm^2 (45 x 45 mm). The column was filled with the transparent soil.

The top of the column was designed to supply a constant head by providing a ponded reservoir. The constant head was restricted in this study to 100 mm maximum height by the overflow port located above the reservoir. The constant head configuration was used to measure the saturated permeability before draining the column.

A zero pressure head boundary applied a constant head to the base of the column. A valve at the base of the column controlled the release of the discharged fluid which was drained into a container and weighed with a digital scale to determine the flow rates.

The side walls of the column have threaded ports (Figure 1b). These ports allow for soil sampling, and can be accommodated for manometers or instrumentation.

The front walls have black circular referenced dots attached at equal separation along the column. These reference dots (Figure 1a) are used for photo analysis and will be discussed in detail later.

2.2 Digital Camera Set-up

Three digital cameras were used to take photos simultaneously during the test (Figure 2). The cameras were located at an equal distance from the column and equal separation between adjacent cameras. The cameras were set at maximum zoom to focus the image on the column and produce the highest quality photos. The separation between cameras was controlled by the minimum overlap of 75 mm required for photo analysis. Three cameras were chosen to reduce the amount of

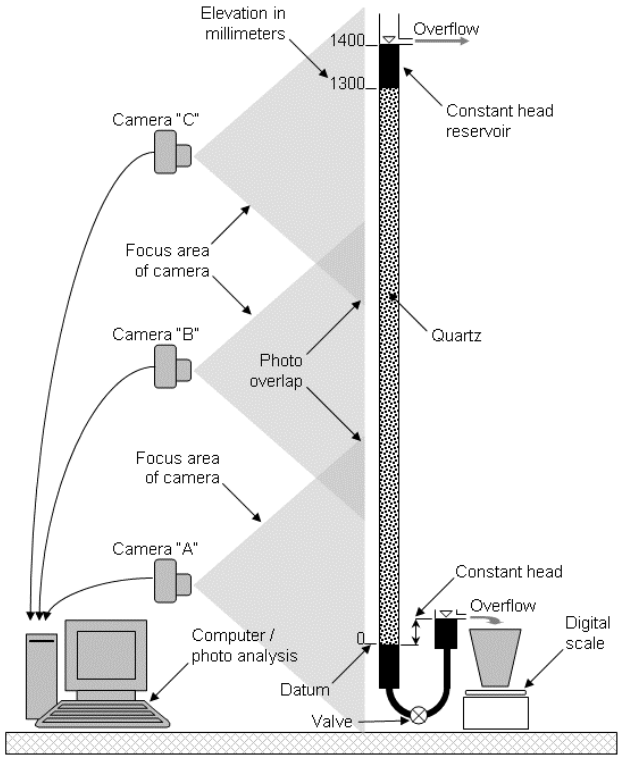

Figure 2. Schematic diagram of transparent soil experimental column apparatus

distortion of images. For this study, the cameras were controlled by the computer to take photographs simultaneously at 6 s intervals throughout the test

3 EXPERIMENTAL PROCEDURE

3.1 Materials Used

The transparent soil used in this study was made by using fused quartz particles and matching the refractive index of the fluid. The transparency of the soil is reliant on the degree of saturation and the precise matching of the refractive indices. Displayed in Figure 1 is the contrast between saturated soil and unsaturated soil to illustrate their particular transparency characteristics.

The soil used in this experiment is a commercially available material and has the ability to represent natural soil particles. The material properties are summarized in Table 1. The soil has an angular particle shape and appears white when dry (Figure 1). The grain size distribution is representative of uniformly graded sand with 100% of its particles smaller then 4.75 mm diameter (Figure 3). A minimum dry density of 1050 kg/m^3 was measured in accordance with ASTM D4254-00.

The fluid was produced by mixing two different white mineral oils to achieve a refractive index of 1.458 to match that of the soil. The fluid's refractive index was adjusted by varying the ratio of each component. An Abbe refractometer was utilized to confirm the target refractive index. All refractive index readings were taken

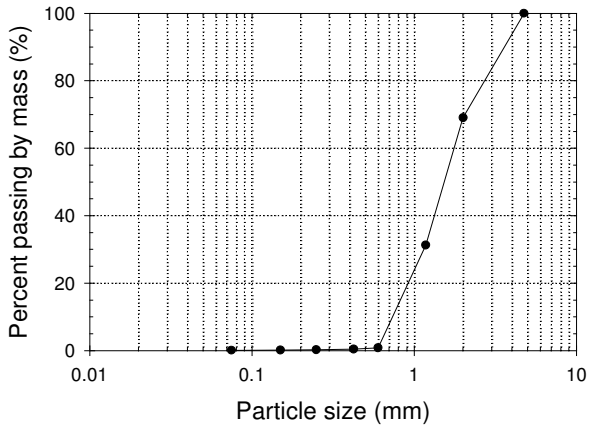

Figure 3. Particle size distribution of transparent soil

at room temperature to avoid any changes in values due to variations in temperature. The fluid mixture resulted in a density of 820 kg/m^3.

3.2 Testing Procedure

The soil was pluviated into the column previously filled with the fluid of matched refractive index. The pluviation technique was employed due to its simple operation, consistency of results and lack of operator influence. In addition, pluviation creates an initially saturated sample with minimal entrapped air bubbles, thus improving the overall transparency of the soil. The soil was placed in 26 equally weighed lifts and the displaced fluid was recorded to determine the as placed density of the soil. A seed particle (Figure 1) of contrasting colour was placed between each lift boundary to observe soil movements.

Table 1. Properties of transparent soil

Parameter	Value
Particle Size Distribution	
- D_{10}	0.73 mm
- D_{30}	1.1 mm
- D_{60}	1.8 mm
- Coefficient of uniformity	2.4
- Coefficient of curvature	1.0
Dry density (as tested)	1130 kg/m^3
Void ratio	1.0
Porosity	49%
Saturated hydraulic permeability	1.6x10^{-3} m/s

Notes: D_{10}, D_{30} and D_{60} = particle diameter corresponding to 10, 30 and 60% by mass of finer particles, respectively

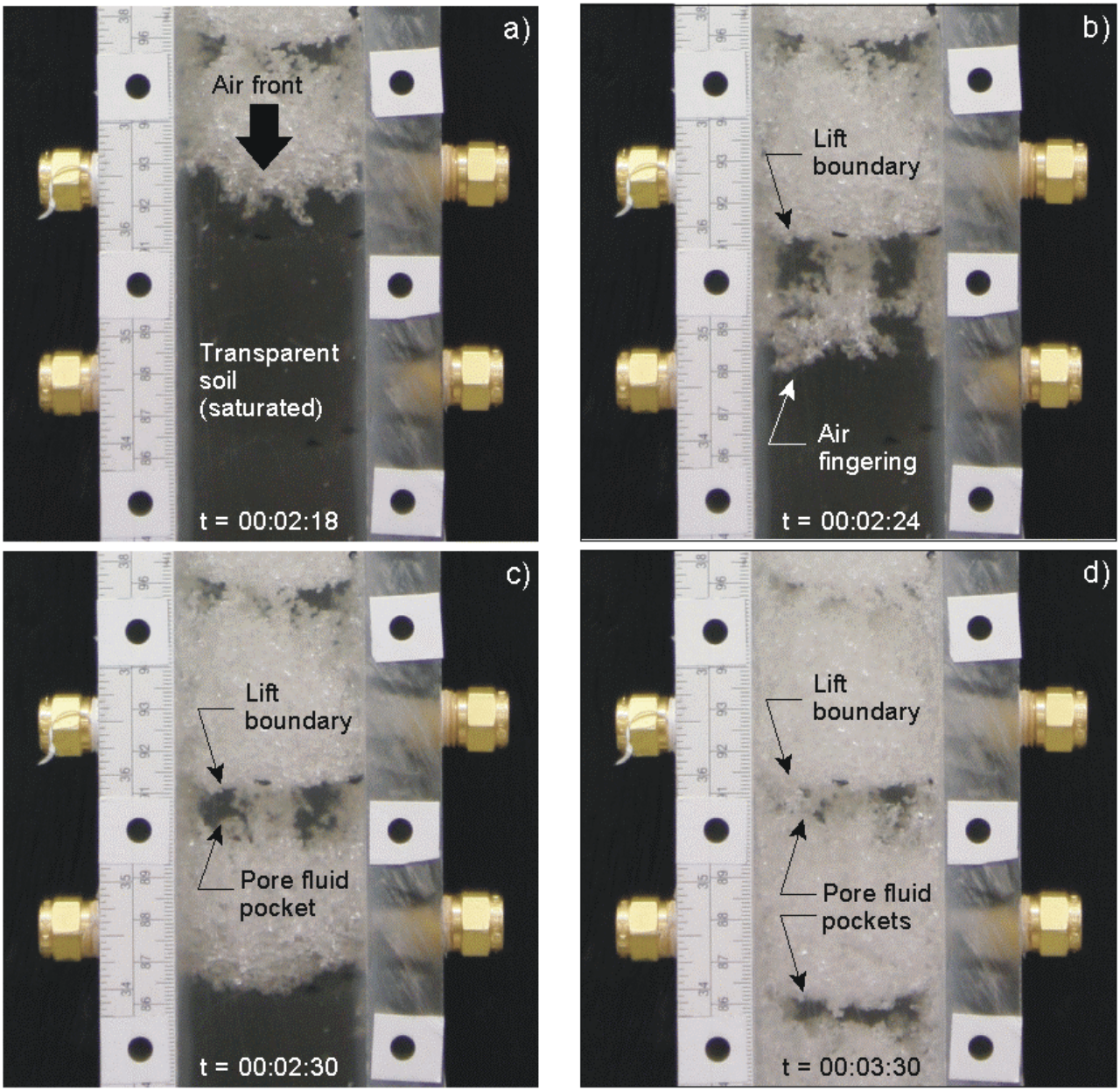

Figure 4. Transition from transparent to non-transparent soil, illustrating: a) advancing air front approaching lift boundary (t = 00:02:18), b) air fingering through lift boundary (t = 00:02:24), c) pocket of fluid trapped at interface of lift boundary (t = 00:02:30), and d) slow dissipation of trapped fluid at interface of lift boundaries (t = 00:03:30)

To decrease the void ratio from its maximum value produced by pluviation, vibratory compaction with a rubber hammer was employed to consolidate the soil to a final density of 1130 kg/m3. The bottom valve on the column was later opened to allow gravity drainage of the fluid.

4 RESULTS

4.1 Photo Interpretation

Shown previously in Figure 1 are two photos ‘a’ and ‘b’ representing saturated and unsaturated transparent soil, respectively. The transition between the saturated and unsaturated state during gravity drainage of the column is shown in Figure 4. All photos shown are from

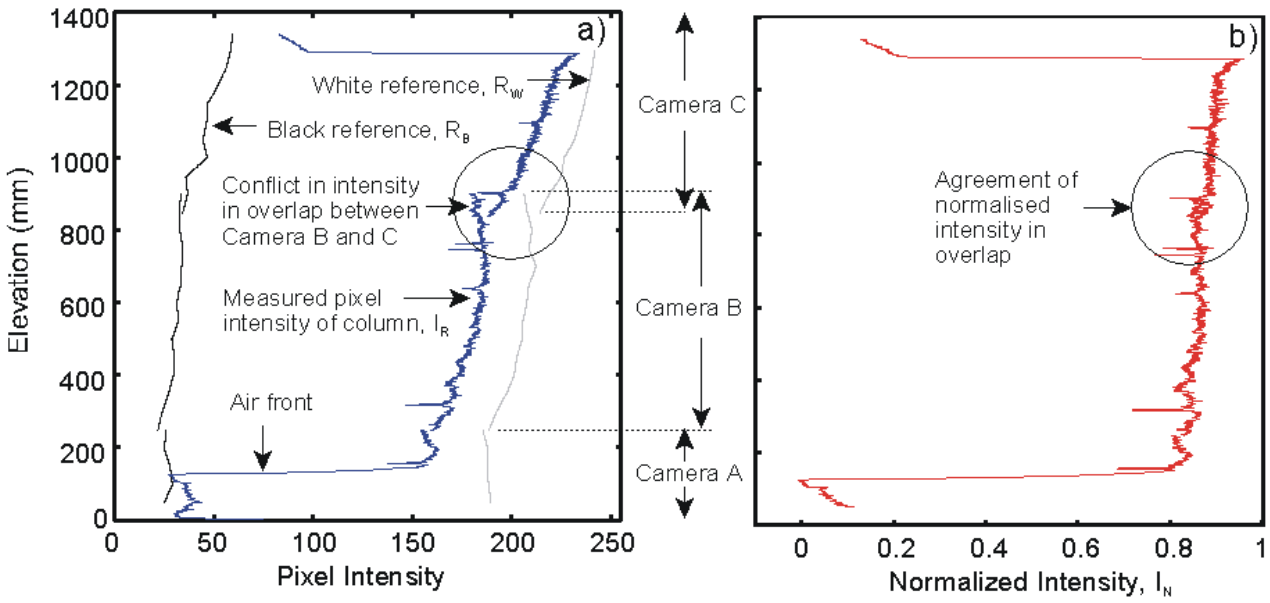

Figure 5. a) Measured pixel intensity over column height at residual fluid content conditions illustrating measured variation in black and white intensity values, and b) calculated normalised pixel intensity

the same position on the column and are centered near 900 mm above the datum. Figures 4a-c are sequential photos taken during the drainage test at 6 s intervals. Figure 4d was taken 1 minute after Figure 4c.

Upon opening the valve at the base of the column (Figure 2), the advancing air front migrated downward. In this study, the advancing air front was defined as the leading edge of the air intrusion which resulted in loss of transparency. The soil behind the air front changes from transparent to non-transparent when the pore fluid is replaced with air. The leading edge of the air front does not travel as a horizontal face at a continuous speed but instead fingers through the column. The speed of travel is locally variable as the air front slows upon reaching a lift boundary then increases in speed after the interface between lifts has been penetrated.

During each pluviated lift, the larger soil particles fell faster than the smaller. The concentration of fines near the top of the lift boundaries, as a result of segregation during pluviation, is evident as seen by the temporary pockets of fluid retention at the lift boundary (i.e. Figure 4c-d). The gradual changes from fine to coarser materials within each lift results in the variable effects that are seen. The sequence of photos shows the delayed dissipation of fluid from the surface of the lift boundaries. The air front migration and delayed dissipation of fluid pockets between lift boundaries was tracked with photo analysis. Without an initially transparent medium, these phenomena would not be visible.

4.2 Photo Analysis

Photo analysis was completed to track the air front migration in the column during a drainage test. The program used tracked the changes in pixel intensities and was modeled after a program developed by White et al. (2003) which tracked soil movements at the particle scale. The initially saturated column appeared black from the background seen through the transparent soil. After de-saturation the soil appeared white in colour after losing its transparency from the intruded air between the pore spaces of the particles (Figure 1 and 4). The black and white colour contrast between saturated and unsaturated soil allows for the ability of photo analysis software to assign values to each and track the advancing air front.

The colours black and white have pixel colour intensity values of 0 and 255, respectively, as plotted along the x-axis in Figure 5a. Since each camera was at a different distance from the main light source above the column, each camera had its own corresponding colour intensity variation. In order to quantify the changing colour intensity, the black dots on the white background (Figure 1) are also used as references along the length of the column. The change in colour intensity is evident in Figure 5a with the decreasing pixel intensity with decreasing column elevation (ie. distance from light source) for both the black and white references. The white and black references are used to normalize the intensity along the column as follows:

$$I_N = \frac{(I_R - R_B)}{(R_W - R_B)} \quad [1]$$

where I_N = normalized intensity, I_R = raw pixel intensity, R_B = black reference and R_W = white reference. The black and white intensity references are specified separately for each elevation and for each camera, thus creating consistency of results between different elevations and cameras. Figure 5b shows an example of

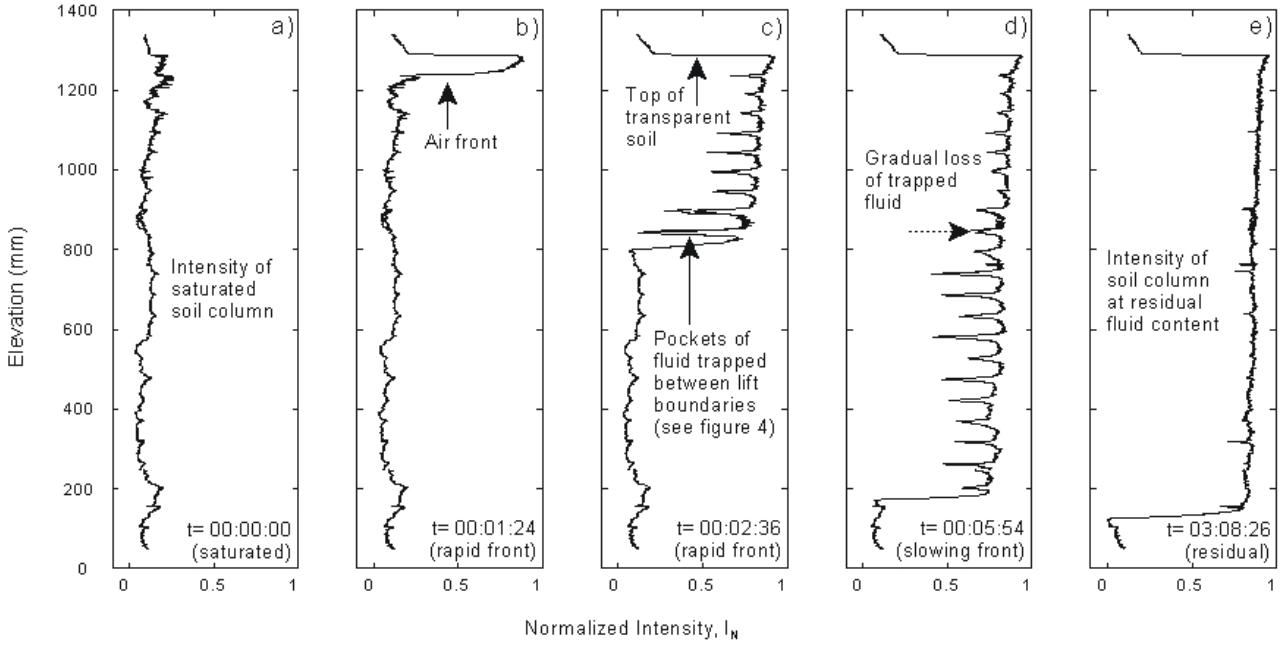

Figure 6. Profiles of normalized intensity during drainage of soil column, illustrating: a) saturated soil, b) beginning of advancing air front, c) advanced air front showing retention of fluid at lift boundaries, d) advancing air front nearing head boundary condition at base of column with gradual loss of entrapped fluid at lift boundaries, and e) residual fluid content of soil column

the agreement in the calculated normalized intensity from raw data. In particular the adjustment of photo overlaps between Cameras "B" and "C" as compared to the conflicting initial raw data of Figure 5a shows good agreement.

4.3 Air Front Migration

The normalized intensity plots for select time intervals during gravity drainage of the column are shown in Figure 6. The saturated condition shown in Figure 6a shows a variation in normalized intensity between 0.04 and 0.2. Since the black reference used is a darker shade then the color of the background behind the column, a non-zero normalized intensity is calculated. Variation of normalized intensity values along the saturated length of the column represent variations in pixel intensity created by minor imperfections of refractive index of the soil and also reflection of light from differences in soil gradations along each pluviated lift. The larger initial normalized intensity values above 1200 mm elevation are the result of entrapped air bubbles produced from the shorter pluviation depth.

The progression of plots in Figure 6 shows the advancement of the air front in the soil transitioning from saturated (Figure 6a) to residual fluid contents (Figure 6e). The air front is plotted by the leading edge of the increase in pixel intensity as labeled in Figure 6b. Figures 6b-d corresponds to the air front migrating along the column. The spikes towards lower pixel intensity values at elevations higher then the air front represent the lift boundary interfaces. Since the fluid in the pore space has momentarily not entirely been replaced by air the soil is still partially transparent resulting in a pixel intensity value between saturated and unsaturated results. The magnitude of the spikes gradually decreases as the residual fluid at the lift boundaries drain with time. When all the lift boundaries have drained and the soil column has reached residual fluid content throughout, the normalized intensity plot becomes linear (Figure 6e).

The air front elevation was mapped at each time-step during the photo analysis process. Figure 7a shows the location of the advancing air front with time as the drainage test progressed. Points B-D on Figure 7a correspond to the air front elevation shown on the profile plots in Figure 6b-d. Initially the air front migrated rapidly at a linear rate through the soil but then decreased in the rate of advancement until it reached a constant elevation provided by the bottom boundary condition at experiment times following point D on Figure 7a.

A similar trend to the air front advancement with time was produced with the fluid outflow rate shown in Figure 7b. Similarly to Figure 7a, points B-E on Figure 7b correspond to plots shown in Figures 6b-e. Figure 7b shows the saturated flow rate produced from the ponded fluid provided by the constant head reservoir (Figure 2). Upon opening of the value at the base of the column to release the fluid, the flow rate decreased to a equilibrium rate less then the saturated rate shown. This constant outflow rate was maintained as the air front migrated through the soil but then gradually decreased as the air front reached the constant head boundary condition provided at the base of the column. Some variations in outflow rate are shown in Figure 7b as the

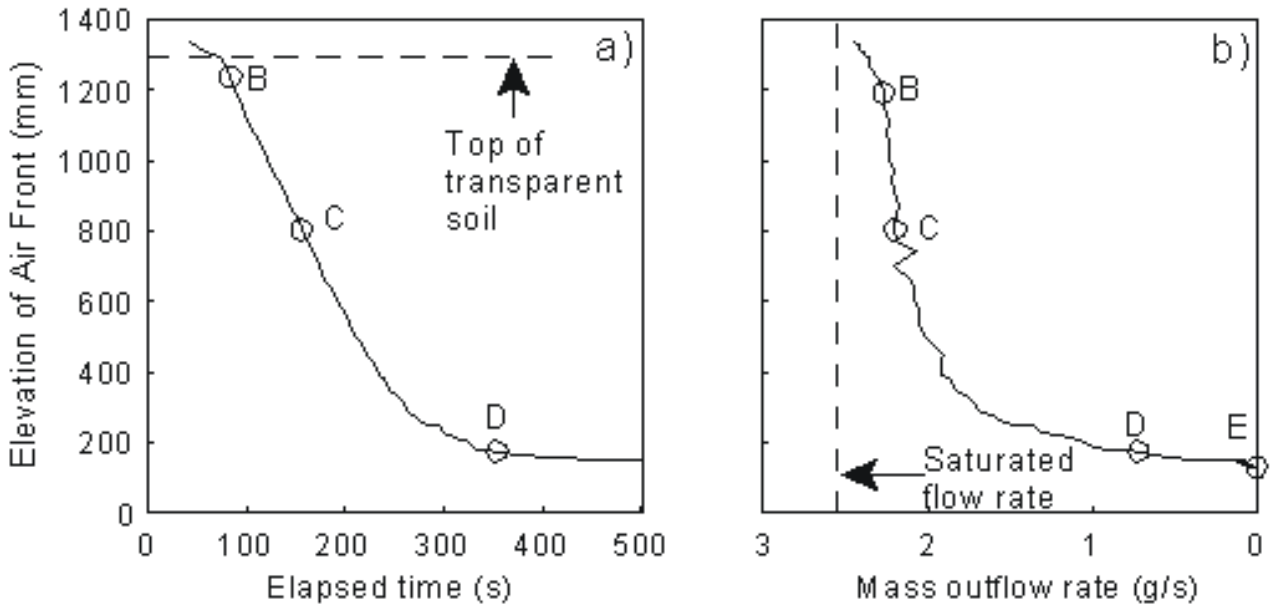

Figure 7. a) Elevation of air front migration through soil column, and b) resulting mass outflow rate of fluid exiting the soil column. Note: Points B-E correspond to profiles in Figure 6

air front momentarily speeds up though the coarser soil particle and then slowed upon reaching the finer soil particles at the top of each pluviated lift boundary. This phenomena is highlighted in Figure 7b following point C of the outflow rate plot.

5 DISCUSSION AND CONCLUSION

A 1-D column apparatus was developed for this study to track the air front migration during gravity drainage of a transparent soil. This experimental data provides a new perspective on air front migration through a granular media. Typical results for a column experiment constructed with lifts of soil initially pluviated through a fluid filled column and then drained are presented in this study. The use of pluviation as a sample preparation method allowed for the segregation of particles and the transparency highlighted the effect of fines at lift boundaries with regard to the retained fluid pockets. The transparency of the soil/fluid combination allowed visual interpretation of the air front in addition to observations of air fingering and preferential flow paths. This phenomenon may help to explain the sometimes inconsistent results of instrumentation installed at different locations within a 1D column apparatus. The use of a transparent soil shows potential in interpreting various unsaturated flow phenomenon that was previously not accurately captured with instrumentation alone.

REFERENCES

Bathurst, R.J., Ho, A.F., Siemens, G. 2007. A Column Apparatus for Investigation of 1D Unsaturated-Saturated Response of Sand-Geotextile Systems. *Geotechnical Testing Journal*, 30(6): 1-9.

Gill, D.R., and Lehane, B.M. 2001. An Optical Technique for Investigating Soil Displacement Patterns. *Geotechnical Testing Journal*, 24(3): 324-329.

Ho, A. 2000. Experimental and Numerical Investigation of Infiltration Ponding in One-Dimensional Sand-Geotextile Columns. M.Sc thesis, Department of Civil Engineering, Queens University, Kingston, ON.

Iskander, M.G., Liu, J. and Sadek, S. 2002. Transparent Amorphous Silica to Model Clay. *Journal of Geotechnical and Geoenvironmental Engineering*, 128(3): 262-273.

Iskander, M.G., Sadek, S., and Liu, J. 2002. Displacement Field Measurement in Transparent Soils. *Engineering Mechanics Conference*, American Society of Civil Engineers.

Iskander, M.G., Sadek, S., and Liu, J. 2002. Optical Measurement of Deformation Using Transparent Silica Gel to Model Sand. *International Journal of Physical Modelling in Geotechnics*, 4: 13-26.

Lo, H.C., Tabe, K., Iskander, M., and Yoon, S.H. Modeling of Mulit-Phase Flow and Sufactant Flushing Using Transparent Aquabeads. *GeoCongress 2008*, American Society of Civil Engineers: 846-853

Lui, J., Iskander, M.G. and Sadek, S. 2003. Consolidation and Permeability of Transparent Amorphous Silica. *Geotechnical Testing Journal*, 26(4): 1-12.

Nahlawi, H., Bouazza, A., and Kodikara, J. 2007. Surface Water Infiltration in a 1-Dimensional Soil-Geotextile Column. *Common Ground Proceedings, 10th Australia New Zealand Conference on Geomechanics*, Brisbane: 368-373.

Sadek, S., Iskander, M.G., and Liu, J. 2002. Geotechnical Properties of Transparent Silica. *Canadian Geotechnical Journal*, 36(1): 111-124.

Stanier, S.A 2007. Geotechnical Modelling Using a Transparent Synthetic Soil. CIV300 Dissertation: Research Paper, 1-5.

Welker, A.L., Bowders, J.J., and Gilbert, R.B. 1999. Applied Reserach Using a Transparent Material with Hydraulic Properties Similiar to Soil. *Geotechnical Testing Journal*, 22(3): 266-270.

White D.J., Take W.A. & Bolton M.D. 2003. Soil deformation measurement using particle image velocimetry (PIV) and photogrammetry. *Geotechnique* 53(7): 619-631.

Yang, H., Rahardjo, H., Wibawa, B., and Leong, E.C. 2004. A Soil Column Apparatus for Laboratory Infiltration Study. *Geotechnical Testing Journal*, 27(4): 1-9.

Yang, H., Rahardjo, H., and Fredlund, D.G. 2004. A Study of Infiltration on Three Sand Capillary Barriers. *Canadian Geotechnical Journal*, 41(4): 629-643.

Yang, H., Rahardjo, H., and Leong, E.C. 2006. Behaviour of Unsaturated Soil Columns during Infiltration. *Journal of Hydrologic Engineering*, 11(4): 329-337.